

1c. NEBULAR EJECTA

IMAGES AND LIGHT CURVES OF THE RADIO REMNANTS OF NOVAE

Robert M. Hjellming
National Radio Astronomy Observatory
Socorro, NM, 87801, USA

Abstract

Radio observations of novae provide direct information about masses, temperatures, and velocities of ejected material, particularly when the radio remnants are resolved or imaged. The radio images of Nova QU Vul 1984 indicate that the mass in its ejecta is $3.6 \cdot 10^{-4} M_{\odot}$, confirming the generally higher masses inferred from radio light curves. All thermally-emitting nova shells that can be observed by the VLA should be resolvable, allowing determination of angular sizes and asymmetries.

1. Introduction

Radio emission has been systematically studied for eight classical novae and one recurrent nova since the first detections of radio emission from HR Del 1967 and FH Ser 1970 by Hjellming and Wade (1970) and Wade and Hjellming (1971). Simple kinematic models were used by Seaquist and Palimaka (1977) to fit the part of the FH Ser data presented in preliminary form by Hjellming (1974); and Kwok (1983) showed that a wind model with a variable mass loss rate could fit the early stages of the FH Ser data before the radio source became optically thin. Hjellming *et al.* (1979) used a "Hubble" flow model to fit all of the phases of the radio light curves for the abovementioned novae and the more extensive radio and infra-red light curves of V1500 Cyg 1975. Since that time Snijders *et al.* (1987) have analyzed the radio light curve of V1370 Aql 1982 and Hjellming *et al.* (1989) have observed the optically thin decay stage of PW Vul 1984 and all stages of the radio light curves of Cyg 1986 and Her 1987. Among the most interesting developments in radio novae in the last ten years were the observations and interpretation of radio emission associated with the imaging of the novae GK Per 1901 and QU Vul 1984 and the recurrent nova RS Oph 1985. The QU Vul radio remnant images have been used to show that the mass of the ejecta is large, $3.6 \cdot 10^{-4} M_{\odot}$. High surface brightness radio emission from QU Vul (early stages) and RS Oph 1985 have been seen, indicating the presence of hot, shocked gas.

II. GK Per 1901 and Non-Thermal Remnants of Novae

Based upon the idea that nova ejecta might be low energy versions of supernova remnants interacting with the interstellar medium, Reynolds and Chevalier (1984) searched for and found an extended, linearly polarized 15" radio remnant associated with GK Per 1901. Seaquist *et al.* (1989) have recently carried out an extensive study of this remnant. Their superposition of a 1.49 GHz image of the remnant and an optical image is shown in Figure 1. One might have hoped that radio remnants like this were

common, but Bode *et al.* (1987) have shown that this behavior is unusual since no other cases have been found; they and Seaquist *et al.* (1989) argue that GK Per was unique because its circumstellar medium is dominated by the neutral remnant of a planetary nebula which was formed about 10^5 years ago.

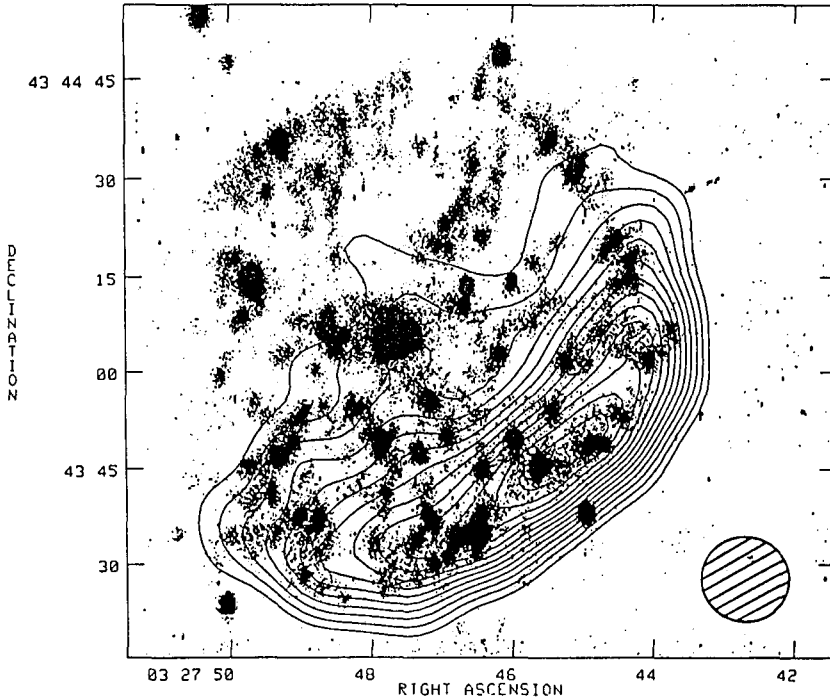


Figure 1 - Optical and 1.49 GHz image of Nova GK Per 1901 remnant.

There is a possibility that non-thermal emission components have been produced with similar interactions with surrounding gas in connection with the anomalous early radio emission of nova QU Vul 1984 (Taylor *et al.* 1987) and the radio remnant of the 1985 outburst of the recurrent nova RS Oph (Padin *et al.* 1985, Hjellming *et al.* 1986). However, the anomalous QU Vul radio emission is most likely to be due to $10^5 - 10^6 K$ shocked gas. In addition to shocked gas seen as high surface brightness components in the RS Oph radio emission there is some evidence for non-thermal emission because of the $10^9 K$ brightness temperatures required by the high resolution VLBI image of Porcas *et al.* (1987). While hot, shocked gas and non-thermal emission components are particularly interesting because of their implications for interactions of nova shells with their environment, let us now concentrate on what direct observations of the radio remnants of classical novae determine about nova ejecta.

III. Radio Light Curves of Radio Novae

Because there has been, up to this time, only two cases in which a nova remnant has been imaged as a resolved radio source, most of the information available about

classical nova radio emission has been due to systematic studies of radio light curves. Figure 2 shows the radio and infra-red light curves of FH Ser 1970 and V1500 Cyg 1975 (Hjellming *et al.* 1979). These are the two best cases in which extensive multi-frequency observations are available which can be fit by a simple model for the evolution of the ejecta of novae. The infra-red data of V1500 Cyg (Ennis *et al.* 1977) fit the same model of a free-free emitting nova shell because it was 200 days or more before the IR emission was "contaminated" by emission from late forming dust. The radio light curves of HR Del 1967, V1370 Aql 1982, Cygni 1986, and Hercules 1987 show the same three "phases" seen in the radio light curves of FH Ser and V1500 Cyg, while PW Vul 1984 was observed only in the third, optically thin phase. It is therefore important to understand the nature of the models that have been used to fit these radio light curves.

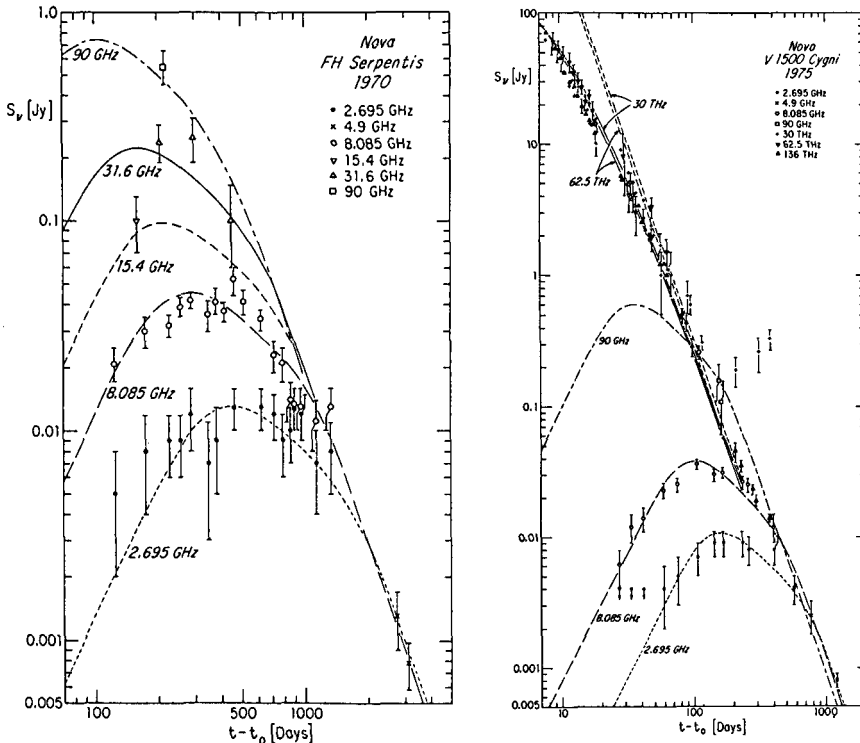


Figure 2 - Radio and infra-red data and model light curves for Nova FH Ser 1970 and Nova V1500 Cyg 1975

The "classical" radio light curves of novae have three phases of evolution. In Figure 3 we show the radio light curves for three radio frequencies using parameters (factor of 1000 velocity gradient) that clearly emphasize these three phases, where the solid curves are for frequencies of 15, 10.6, and 7.5 GHz, and the dashed curves are exact or approximate formulas for the dominant emission components in the three phases. In phase I the radio emission shows an increase due to the expansion of an optically thick pseudo-photosphere coincident with the outer parts of the nova ejecta, so the radio flux is proportional to $\nu^2 \cdot t^2$, where ν is the frequency and t is the time since outburst. There

is then a transition period during which the light curves go through a maximum while evolving to a phase II dominated by the optically thick emission of a radio pseudo-sphere which occurs at progressively smaller fractions of the shell radius as the shell expands, leading to a dominant radio emission component proportional to $\nu^{0.6} \cdot t^{-4/3}$. Phase II can be very short if there are negligible velocity gradients across the shell, but it can be very long if there is a very large velocity gradient or, equivalently, the ejecta behave like a variable stellar wind with $\dot{m} \approx R_2^{-1}$, where R_2 is linearly proportional to time. In fact, the clearest evidence for termination of ejection of a “Hubble” flow shell or variable wind is the fact that all radio light curves of novae either quickly, or eventually, make a transition to an optically phase III where the free-free emission flux densities are proportional to $\nu^{-0.1} \cdot t^{-3}$.

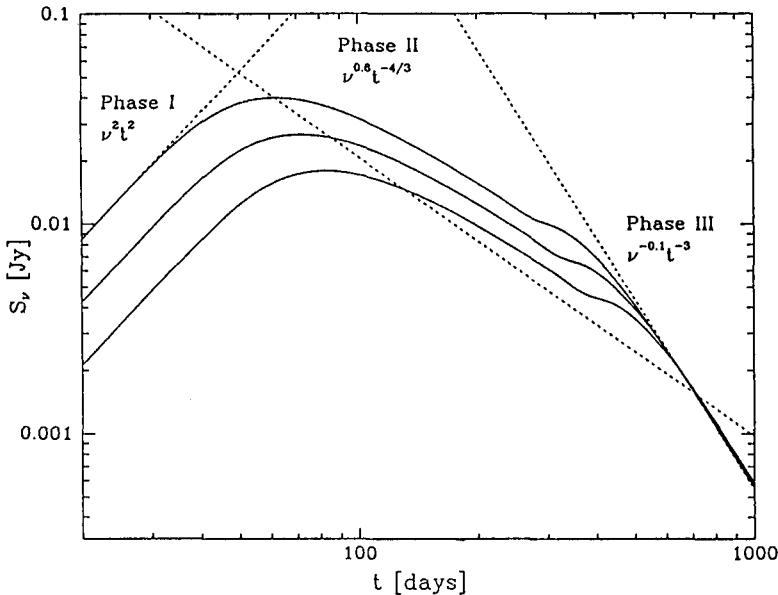


Figure 3 - Radio light curves (solid lines) showing phases I (optically thick), II (receding photosphere), and III (optically thin) for 15, 10.6, and 7.5 GHz.

In order to understand the information about nova ejecta that is provided by radio light curves, let us discuss the simple kinematic models that have previously been used to fit radio and optical light curves, and then discuss a “unified” kinematic model that includes all the important features of these models, and which can be used to fit the radio data for all novae exhibiting phase I, II, and III light curves. Figure 4 shows first the “Hubble” flow model in which a spherically symmetric shell is suddenly ejected with mass M , uniform electron temperature T_e , and initial inner and outer radii R_{10} and R_{20} , with the shell having a constant velocity gradient from inner to outer parts with v_1 and v_2 as constant inner and outer velocities. As shown in Figure 4, this model requires that $v_2 > v_1$ and leads a simple formula for the density, $\rho(R, t) = [1/(4\pi R^2)] \cdot M/[R_2(t) - R_1(t)]$, in the shell. Kwok (1983) showed that an optically thick wind model with variable mass loss rate fits the phase I and II behavior of FH Ser. This model is the same as the optically thick wind model used to calculate optical

light curves of novae (Harwick and Hutchings, 1978) who assumed $\dot{m} \approx R_2^{-1}$ at an inner layer $R_1 = R_{10}$, and this leads to $\rho(R, t) = [1/(4\pi R^2)] \cdot [M/R_2(t)]$ in the shell density. These two models make different assumptions during the derivation of the density distribution, but have the same mathematical result if one can ignore the effects of a finite inner radius. As mentioned earlier, the fact that all radio novae evolve from the optically thick photosphere phase II to a finite, optically thin remnant means that one must terminate the wind or shell ejection. The right hand side of Figure 4 shows a “unified” model that incorporates the essential features needed to fit all the major radio and optical light curve characteristics of nova shells. The outer radius expands with a constant velocity v_2 , however the inner radius does not begin expanding with velocity v_1 time t_s . The density then varies in the shell as prescribed for the Hubble flow model and the behavior of inner and outer radii is a compromise with the essential features of both Hubble flow and variable wind models.

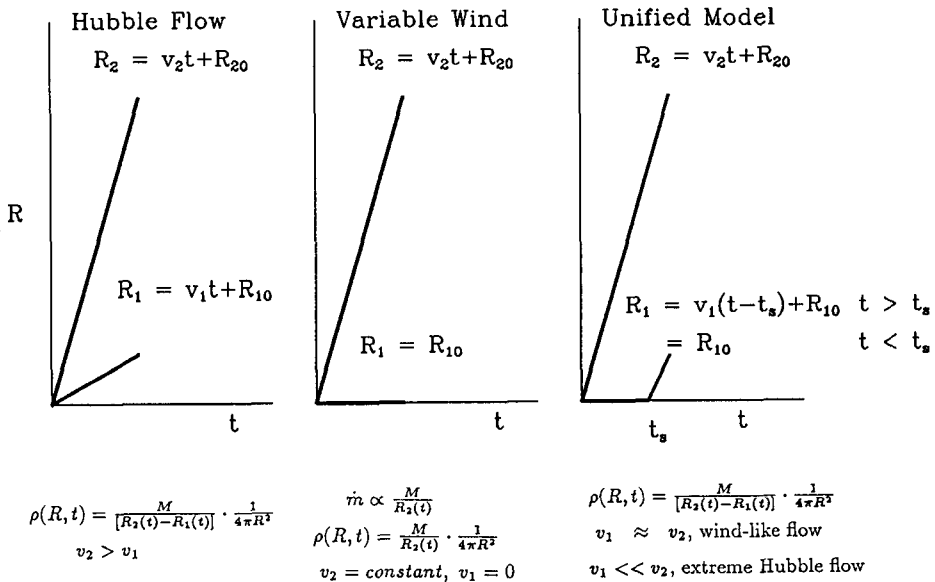


Figure 4 - Schematic illustrations and equations for the “Hubble flow”, variable wind, and “unified” kinematic models for nova shells

The free-free emission, “unified” model can be summarized as follows. We define an angular radius parameter,

$$\theta_{ff} = \left(\frac{0.133}{d_{kpc}} \right) \left(\frac{M}{10^{-4} \mu M_{\odot}} \right)^{-0.4} \left(\frac{T_e}{10^4 K} \right)^{-0.268} \left(\frac{\nu_{GHz}}{15} \right)^{-0.42} \quad \text{arcsec}$$

where μ is the mean molecular weight, d_{kpc} is the distance in kpc, and ν_{GHz} is the frequency in GHz. Defining $\theta = R/d$ and $x = \theta/R_2(t)$, and letting all subsequent

θ 's be in units of arcseconds, the radio emission for a spherically symmetric, constant temperature nova shell is given by the flux density

$$S_\nu(t) = 10.12 \cdot \theta_2^2(t) \left(\frac{T_e}{10^4 K} \right) \left(\frac{\nu_{GHz}}{15} \right)^2 \cdot \int_0^1 x \cdot (1 - e^{-\tau_\nu(x,t)}) dx \quad Jy$$

where

$$\tau_\nu(x,t) = \frac{\theta_{ff}^5}{[(1 - \theta_1(t)/\theta_2(t))^2 \theta_2^2(t) [G(x, x_1) - \delta(x \leq x_1)G(x, 1)]},$$

if one also defines

$$G(x, x_1) = \left(\frac{1}{x^2} \right) \left(\frac{(x_1^2 - x^2)^{0.5}}{x_1^2} \right) + \left(\frac{1}{x} \right) \cos^{-1} \frac{x}{x_1}$$

and $\delta(x \leq x_1) = 1$ if $x \leq x_1$, and $= 0$ if $x > x_1$. From these equations the optically thick and thin limits for the radio flux density are

$$S_{\nu,thick}(t) = 5.06 \cdot \theta_2^2(t) \left(\frac{T_e}{10^4 K} \right) \left(\frac{\nu_{GHz}}{15} \right)^2 \quad Jy$$

and

$$S_{\nu,thin}(t) = 10.12 \left(\frac{\theta_{ff}^5}{[\theta_2(t) - \theta_1(t)]\theta_1(t)\theta_2(t)} \right) \quad Jy.$$

The only simple case for which the contribution of the receding optically thick pseudo-photosphere at $x = x_{ph}$ can be calculated analytically is in the extreme where $x_1 \ll 1$ and $G(x_{ph}, x_1) = 0.5 \cdot \pi/x_{ph}^3$ so

$$S_{\nu,ph}(t) \approx S_{\nu,thick}(t) \left(\frac{3\pi}{4} \left(\frac{\theta_{ff}^5}{[\theta_2(t) - \theta_1(t)]^2 \theta_2^3} \right) \right)^{2/3}$$

leading to the result that $S_{\nu,ph} \propto \nu^{0.6} \cdot t^{-4/3}$.

What are the masses and inner and outer velocities needed to fit the radio, optical, and infra-red data? The following table gives the results for three novae obtained by Hjellming *et al.* (1979) and Hartwick and Hutchings (1978). The radio-determined parameters are as defined before, and their equivalents when derived from optical data, are designated $M_{optical}$ and $v_{optical}$. The distances for HR Del, FH Ser, and V1500 Cyg are assumed to be 0.8, 0.65, and 1.4 kpc.

Table 1 – Parameters Determined from Radio vs Optical Data

Name	$M \left(\frac{T_e}{10^4} \right)^{0.58}$ [M_\odot]	$v_2 \left(\frac{T_e}{10^4} \right)^{0.5}$ [km/sec]	$\frac{v_1}{v_2}$	$M_{optical}$ [M_\odot]	$v_{optical}$ [km/sec]
HR Del	$8.6 \cdot 10^{-5}$	450	0.44	$1.3 \cdot 10^{-5}$	550
FH Ser	$4.5 \cdot 10^{-5}$	1000	0.05	$1.0 \cdot 10^{-5}$	700
V1500 Cyg	$2.4 \cdot 10^{-4}$	5600	0.036	$1.8 \cdot 10^{-5}$	2070

However, these quantities scale with an undetermined temperature. In addition, the masses one determines assuming $T_e = 10^4 K$ are a factor of ten to fifteen higher than often inferred from optical or UV diagnostics, and the velocities are often a factor of two larger. This may be because the radio light curves reflect emission ranging from the least dense, high velocity outer layers inward to the denser layers which dominate emission processes weighted by ρ^2 . Indeed, shortly after radio maximum the observed emission comes from a rapidly decreasing fraction of the total mass in the ejecta. The problem of discrepancies in determinations from different sources of data will be understood only when care is taken to fit the same models to all sources of data. However, most of the ambiguities in radio determinations disappear when one can image or resolve the nova ejecta.

IV. Imaging or Resolving Nova Shells

The first images of the radio remnant of a classical nova, caused by thermal emission from its shell, were obtained for nova QU Vul 1984 (Taylor *et al.* 1987, 1988). As shown in Figure 5, the shell evolved from an apparent bipolar morphology to a roughly circularly symmetric shell with a decrease of intensity in the center. The anomalously strong emission seen early in its lifetime (Taylor *et al.* 1987) was probably due to a very hot, shocked gas component that gave surface brightnesses of the order of a few hundred thousand degrees, and somewhat higher surface brightnesses remained 497 days after outburst with the bipolar morphology shown in the first image in Figure 5. However,

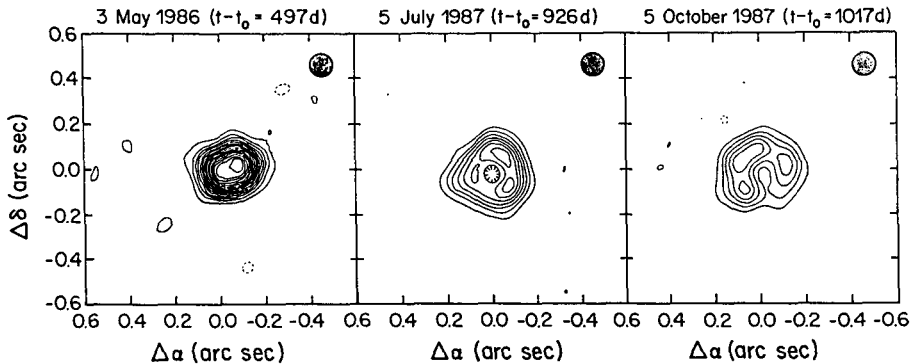


Figure 5 - Three epochs of VLA Images of the QU Vul nova shell at 14.9 GHz

by 926 and 1017 days after outburst only lower surface brightness components were present. As discussed by Taylor *et al.* (1988) the last two epochs of images are easily fit by the model discussed earlier with $T_e = 17000K$, $M = 3.6 \cdot 10^{-4} M_\odot$ for $\mu = 1.2$, $v_1 = 880$ km/sec, and $v_2 = 1010$ km/sec. The observed size scale seen in Figure 5 is consistent with the angular size determined from infra-red, masked speckle observations by Greenhouse *et al.* (1989). The later images of QU Vul indicate that the shell became spherically symmetric, and the measured surface brightness and size determines the average temperature and the other parameters of the model. If μ is larger because of higher abundances of heavy metals, the mass will decrease, but if there is sub-clumping

in the shell, the mass increases. Thus the relatively high mass obtained for the QU Vul shell supports the larger mass scale indicated by the other radio novae discussed earlier.

The free-free emitting radio remnant of QU Vul could be imaged because it maintained high surface brightness, corresponding to brightness temperatures ≥ 1000 K, during the three years needed for velocities of the order of 1000 km/sec to produce angular radii of $0.15''$. Why does this not happen with more novae? Figure 6 shows models of 14.9 GHz surface brightness evolution, in the form of brightness temperature ($T_b = T_e[1 - \exp(-\tau_\nu)]$) vs θ for V1500 Cyg for $t = 10, 30, 50, 100, 150, 250, 400, 600,$ and 1000 days after outburst. The solid curves correspond to the period when the flux density is increasing while the dashed curves correspond to the peak and decay of the light curves. The extent to which one resolves or images a shell depends on the angular size scales for the higher brightness temperature components of the emission. These scales are determined by $\theta_2(t) = 0.2''(v_2/1000 \text{ km sec}^{-1}) \cdot t_{yr}/d_{kpc}$, $\theta_1(t) = 0.2''(v_1/1000 \text{ km sec}^{-1}) \cdot (t_{yr} - t_{s,yr})/d_{kpc}$ (for $t > t_s$), and, most importantly the radius of the pseudo-photosphere which can be approximated by

$$\theta_{ph}(t) \approx 0.2 \cdot \nu_{GHz}^{-0.7} \left(\frac{T_e}{10^4 K} \right) \left(\frac{M}{10^{-4} \mu M_\odot} \right) \cdot d_{kpc}^{-5/2} [\theta_2(t) - \theta_1(t)]^{-2/3} \text{ arcsec}$$

which sets the size scale of the dominant emission near and after radio maximum. Once $\theta_{ph} \leq \theta_1$ the surface brightness changes from roughly T_e at the pseudo-photosphere in phase II to an optically thin phase III where it decays roughly as t^{-2} . There is a time, t_m , when flux density and the angular size of the photosphere are both at a maximum, that can be determined by solving for the time when $S_{\nu,ph} = S_{\nu,thick}$ (cf. Figure 3), and $t_m \approx [(3\pi/4)/(1 - v_1/v_2)^2]^{0.2} \cdot R_{ff}/v_2$. Any nova that can be detected with good signal to noise can be resolved. This result is well known for thermal emission of stellar winds, and it should have been realized more than ten years ago that strong novae should be resolvable, at or around radio maximum, with high resolution radio interferometers. Let q be the distance between antennas, in units of wavelengths, so the 36 km VLA operating at 14.9 GHz will have values of q as large as $1.8 \cdot 10^6$ wavelengths. The visibility function for a spherically symmetric "unified" model is given by

$$V_\nu(q) = 10.12 \cdot \theta_2^2(t) \left(\frac{T_e}{10^4 K} \right) \left(\frac{\nu_{GHz}}{15} \right)^2 \int_0^1 x \cdot J_0 \left(\frac{2\pi q x \theta_2(t)}{206265} \right) \cdot [1 - e^{-\tau_\nu(x,t)}] dx \text{ Jy.}$$

In Figure 7 we show the visibility functions for the model that fits the radio and infra-red light curve data of V1500 Cyg for $t = 10, 30, 50, 100, 150, 250, 400, 600,$ and 1000 days. The abscissa maximum in Figure 7 is $1.8 \cdot 10^6$ wavelengths, corresponding to the 36 km VLA at 14.9 GHz. Measuring visibility functions with sufficient signal to noise should allow one to study changes in angular size and structure. Most importantly, visibility profiles at different position angles will allow measurements of asymmetries that appear in the ejecta. From Figure 6 we see that it is the decrease of surface brightness beyond angular radii of about $0.1''$ that makes it difficult to image most novae. However, novae attaining flux densities of a few mJy or more at 14.9 GHz, which may not be imageable, will have measurable, two-dimensional visibility functions which, with radio light curves, will allow unambiguous determinations of nova ejecta parameters.

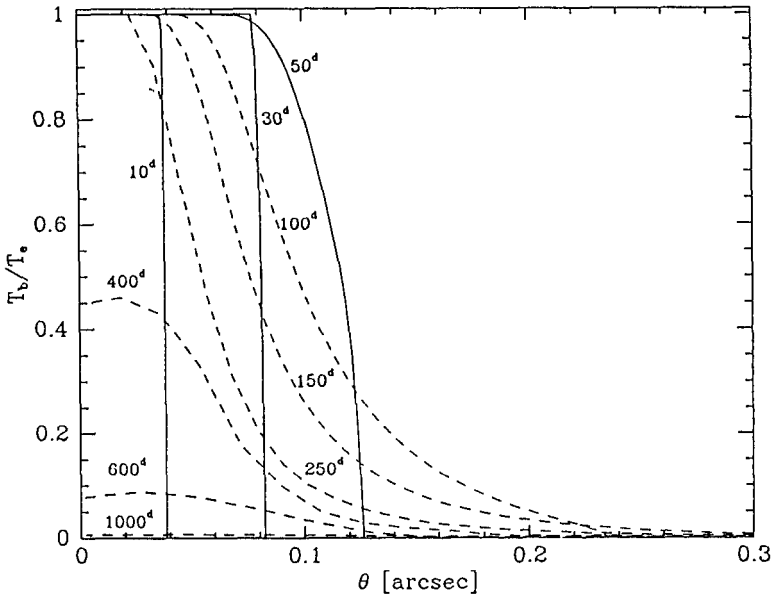


Figure 6 - Brightness temperature (T_b) vs θ at 14.9 GHz for V1500 Cyg at $t = 30, 50, 100, 150, 250, 400, 600,$ and 1000 days

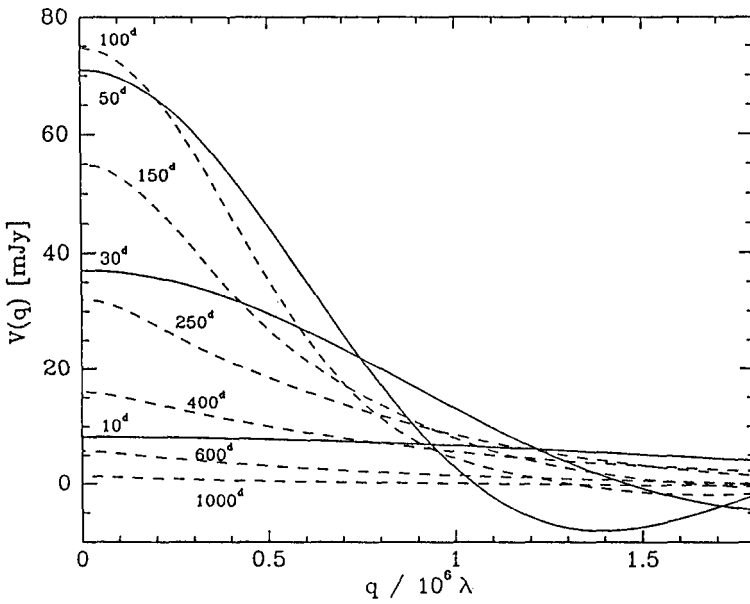


Figure 7 - $V_\nu(t)$ vs q (in wavelengths) at 14.9 GHz for V1500 Cyg at same t as Figure 6.

V. Conclusions

Classical novae which emit significant free-free emission at high radio frequencies can (at or shortly after radio maximum), be imaged, or have angular sizes and asymmetries determined from visibility functions measured with high resolution arrays like the VLA. These measurements, when used with multi-frequency radio (and sometimes infra-red) data, should resolve the basic problem of generally higher mass and velocity determinations, and allow one to study asymmetries in ejecta geometry. QU Vul 1984 images are fit by models that generally support the higher masses and velocities. The radio light curves at different epochs, and final optically thin images, are probably complete observations of ejecta. It most important to understand how data from different wavelength regimes fit together in "unified" models (including asymmetries if warranted by the data) such as we have discussed for optical, infra-red, and radio light curves, but much more extensive fitting to other sources of data remains to be done.

The National Radio Astronomy Observatory is operated by Associated Universities, Inc. under a cooperative agreement with the National Science Foundation.

References

- Bode, M.F., Seaquist, E.R., and Evans, A. 1987, *M.N.R.A.S.*, **228**, 217.
 Ennis, D., Becklin, E.E., Beckwith, S., Elias, J., Gatley, I., Matthews, K., and Neugebauer, G. 1977, *Ap.J.*, **214**, 478.
 Greenhouse, M.A. *et al.* 1989, *Ap. J.*, in press.
 Hartwick, F.D.A. and Hutchings, J.B. 1978, *Ap.J.*, **226**, 203.
 Hjellming, R.M. 1974, *In Galactic and Extra-Galactic Radio Astronomy, 1st Ed.*, Ed. K. Kellermann and G. Verschuur (Springer-Verlag, New York), p. 159.
 Hjellming, R.M. *et al* 1989, *Ap.J.*, in preparation.
 Hjellming, R.M. and Wade, C.M. 1970, *Ap.J.(Letters)*, **162**, L1.
 Hjellmng, R.M., van Gorkom, J.H., Taylor, A.R., Seaquist, E.R., Padin, S., Davis, R.J., and Bode, M.F. 1986, *Ap.J.*, **305**, L71.
 Hjellming, R.M., Wade, C.M., Vandenberg, N.R., and Newell, R.T. 1979, *A.J.*, **84**, 1619.
 Kwok, S. 1983, *M.N.R.A.S.*, **202**, 1149.
 Reynolds, S.P. and Chevalier, R.A. 1984, *Ap.J.(Letters)*, **281**, L33.
 Padin, S., Davis, R.J., and Bode, M.F. 1985, *Nature*, **315**, 306.
 Porcas, R.W. *et al.* 1987, *In "RS Ophiuchi (1985) and the Recurrent Nova Phenomena*, ed. M.F. Bode (UNV Science Press, Utrecht), p. 203.
 Seaquist, E.R., Bode, M.F., Frail, D.A., Roberts, J.A., Evans, A., and Albinson, J.S. 1989, *Ap.J.* (in press).
 Seaquist, E.R. and Palimaka, J. 1977, *Ap.J.*, **217**, 781.
 Snijders, M.A.J. *et al.* 1987, *M.N.R.A.S.*, **228**, 329.
 Taylor, A.R., Seaquist, E.R., Hollis, J.M., and Pottasch, S.R. 1987, *Astr. Ap.*, **183**, 38.
 Taylor, A.R., Hjellming, R.M., Seaquist, E.R., and Gehrz, R.D. 1988, *Nature*, **335**, 235.
 Wade, C.M. and Hjellming, R.M. 1971, *Ap.J.(Letters)*, **163**, L65.